






Article

Chrysoberyl and associated beryllium minerals resulting from metamorphic overprinting of the Maršíkov–Schinderhübel III pegmatite, Czech Republic

Olena Rybnikova^{1*}, Pavel Uher¹, Milan Novák², Štěpán Chládek³ , Peter Bačík¹ , Sergii Kurylo⁴ 
and Tomáš Vaculovič^{5,6}

¹Department of Mineralogy, Petrology and Economic Geology, Faculty of Natural Sciences, Comenius University, Ilkovičova 6, 842 15 Bratislava, Slovakia; ²Department of Geological Science, Faculty of Science, Masaryk University, Kotlářská 267/2, 611 37 Brno, Czech Republic; ³Department of Geological Engineering, Faculty of Mining and Geology, VŠB – Technical University of Ostrava, 17. listopadu 15, 708 33 Ostrava, Czech Republic; ⁴Earth Science Institute, Slovak Academy of Sciences, Ďumbierska 1, 974 11 Banská Bystrica, Slovakia; ⁵Department of Chemistry, Faculty of Science, Masaryk University, Kotlářská 267/2, 611 37 Brno, Czech Republic; and ⁶Institute of Laboratory Research on Geomaterials, Faculty of Natural Sciences, Comenius University, Ilkovičova 6, 842 15 Bratislava, Slovakia

Abstract

The Maršíkov–Schinderhübel III pegmatite in the Hrubý Jeseník Mountains, Silesian Domain, Czech Republic, is a classic example of chrysoberyl-bearing LCT granitic pegmatite of beryl–columbite subtype. This thin pegmatite dyke, (up to 1 m in thickness in biotite–amphibole gneiss is characterised by symmetrical internal zoning. Tabular and prismatic chrysoberyl crystals (≤ 3 cm) occur typically in the intermediate albite-rich unit and rarely in the quartz core. Chrysoberyl microtextures are quite complex; their crystals are irregularly patchy, concentric or fine oscillatory zoned with large variations in Fe content (1.1–5.3 wt.% Fe_2O_3 ; ≤ 0.09 apfu). Chrysoberyl compositions reveal dominant $\text{Fe}^{3+} = \text{Al}^{3+}$ and minor $\text{Fe}^{2+} + \text{Ti}^{4+} = 2(\text{Al}, \text{Fe})^{3+}$ substitution mechanisms in the octahedral sites. Tin, Ga, and V (determined by LA-ICP-MS) are characteristic trace elements incorporated in the chrysoberyl structure, whereas anomalously high Ta and Nb concentrations (thousands ppm) in chrysoberyl are probably caused by nano- to micro-inclusions of Nb–Ta oxide minerals; especially columbite–tantanite. Textural relationships between associated minerals, distinct schistosity of the pegmatite parallel to the host gneiss foliation and fragmentation of the pegmatite body into blocks as a result of superimposed stress are clear evidence for deformation and metamorphic overprinting of the pegmatite. Primary magmatic beryl, albite and muscovite were transformed to chrysoberyl, fibrolitic sillimanite, secondary quartz and muscovite during a high-temperature ($\sim 600^\circ\text{C}$) and medium-pressure (~ 250 – 500 MPa) prograde metamorphic stage under amphibolite-facies conditions. A subsequent retrograde, low-temperature (~ 200 – 500°C) and pressure (≤ 250 MPa) metamorphic stage resulted in the local alteration of chrysoberyl to secondary Fe,Na-rich beryl, euclase, bertrandite and late muscovite.

Keywords: chrysoberyl, beryl, euclase, bertrandite, sillimanite, granitic pegmatite, metamorphic overprint

(Received 24 January 2023; accepted 23 March 2023; Accepted Manuscript published online: 30 March 2023; Associate Editor: Edward Sturgis Grew)

Introduction

Chrysoberyl, ideally BeAl_2O_4 , is an oxide mineral of olivine-type structure with Be^{2+} cations in tetrahedral and Al^{3+} in octahedral coordination. The main substituents of Al^{3+} are Cr^{3+} (mariinskite BeCr_2O_4 , a Cr-dominant member; Pautov *et al.*, 2013) and Fe^{3+} (up to ~ 6 wt.% Fe_2O_3 , Žáček and Vrána, 2002). Alexandrite, a gemstone variety of chrysoberyl, is characterised by two distinct optical effects, including the alexandrite effect produced by Cr^{3+} and V^{3+} impurities and the cat's eye effect. Three principal lithological types of magmatic or metamorphic chrysoberyl occurrences have been recognised: (1) granitic pegmatites and exceptionally leucogranites; (2) metasomatic skarn zones and related dykes

along/near the contacts between ultrabasic or carbonate rocks and intruded granites to pegmatites; and (3) high-temperature metamorphic rocks of granulite facies (e.g. Martin-Izard *et al.*, 1995; Barton and Young, 2002; Downes and Bevans, 2002; Černý, 2002; Franz and Morteani, 2002; Marschall and Walton, 2014).

Chrysoberyl has been described as an accessory mineral in numerous rare-element, peraluminous granitic pegmatites of the beryl type or, rarely, in pegmatites of the abyssal class (Grew, 1981; Černý and Ercit, 2005; Cempírek and Novák, 2006). Chrysoberyl is usually associated with primary rock-forming minerals such as quartz, feldspars and muscovite, and locally with beryl. However, the origin of chrysoberyl in granitic pegmatites is typically uncertain: it is considered to be a product of primary magmatic precipitation or metamorphic overprinting of a parental pegmatite. A primary magmatic origin for chrysoberyl is suggested for pegmatites in Southern Kerala, India (Soman and Nair, 1985), the Malga Garbella pegmatite, Italy (Vignola *et al.*, 2018), Tablada I pegmatite, Argentina (Colombo *et al.*, 2021) and the Tashisayi pegmatites,

*Corresponding author: Olena Rybnikova; Email: rybnikovageochem95@gmail.com

Cite this article: Rybnikova O., Uher P., Novák M., Chládek Štěpán, Bačík P., Kurylo S. and Vaculovič T. (2023) Chrysoberyl and associated beryllium minerals resulting from metamorphic overprinting of the Maršíkov–Schinderhübel III pegmatite, Czech Republic. *Mineralogical Magazine* 87, 369–381. <https://doi.org/10.1180/mgm.2023.22>

China (Hong *et al.*, 2021). Magmatic chrysoberyl in assemblage with beryl, sillimanite and gahnite was described from the highly-evolved, peraluminous Belvís de Monroy leucogranite, Spain (Merino *et al.*, 2013). However, most occurrences of chrysoberyl consider it to have formed from the breakdown of primary beryl as a result of metamorphic overprinting of the pegmatite e.g. Kolsva, Sweden; Haddam, USA; and Maršíkov, Czech Republic (Franz and Morteani, 1984, 2002; Černý *et al.*, 1992); Kalanga Hill, Zambia (Žáček and Vrána, 2002); Ethel Mary and Viorco, Argentina (Lira and Sfragulla, 2011; Galliski *et al.*, 2012); New York, USA (Lupulescu *et al.*, 2012); Roncadeira, Brazil (Beurlen *et al.*, 2013); and Mt. Begbie, Canada (Dixon *et al.*, 2014).

In this investigation we examine the composition of chrysoberyl and associated minerals at the Maršíkov-Schinderhübel III granitic pegmatite, the first reported occurrence of chrysoberyl in Europe (Hruschka, 1824). The principal objectives of our study were to characterise textural, paragenetic and compositional relations of chrysoberyl and associated Be minerals, and to estimate the conditions of formation of assemblages containing these minerals, and to relate these to the metamorphic evolution of the pegmatites.

Regional geology and pegmatite description

The granitic pegmatite occurs in the Desná Dome, Neoproterozoic to Devonian crystalline basement of the Silesian Domain of Bohemian Massif, a part of the European Variscan

orogenic belt (Fig. 1). The Silesian Domain represents an orogenic wedge belonging to the Moravo-Silesian Zone, a metamorphosed and imbricated margin at the eastern Variscan front in NE Bohemian Massif (Schulmann and Gayer, 2000; Schulmann *et al.*, 2014). The central part of the Desná Dome consists of orthogneisses, paragneisses and amphibolites showing Neoproterozoic protolith ages (570–650 Ma; Kröner *et al.*, 2000; Jastrzębski *et al.*, 2021) and Palaeozoic cover rocks, mainly metaquartzites, metaconglomerates, metapelites and marbles, which are intruded locally by Middle Devonian (Givetian) volcanic rocks of arc and back-arc affinity (Janoušek *et al.*, 2014). This metamorphic complex underwent Variscan medium-pressure, Barrovian-type metamorphism at $P \approx 500\text{--}700$ MPa and $T \approx 540\text{--}660^\circ\text{C}$ (Souček, 1978; René, 1983; Cháb *et al.*, 1990; Schulmann and Gayer, 2000; Košuličová and Štípská, 2007; Schulmann *et al.*, 2014).

The metamorphic rocks were intruded by Variscan, Carboniferous to Early Permian granitic rocks and pegmatites. Zircon U–Pb radiometric age determination of pegmatitic leucogranite at Čertovy Kameny hill near Jeseník gave 334 Ma (Hegner and Kröner, 2000), which is consistent with ages of older granitic plutons in the adjacent Sudetic block of NE margin of the Bohemian Massif: Kłodzko-Złoty Stok, Jawornik, Strzelin, and Kudowa plutons (350–330 Ma; Mikulski *et al.*, 2013). Moreover, a younger plutonic suite of I-type granodiorites to granites of the Žulová Pluton have late-Variscan, Early Permian emplacement ages of 292 ± 4 or 291 ± 5 Ma (LA-ICP-MS U–Pb zircon radiometric age determination; Laurent *et al.*, 2014).

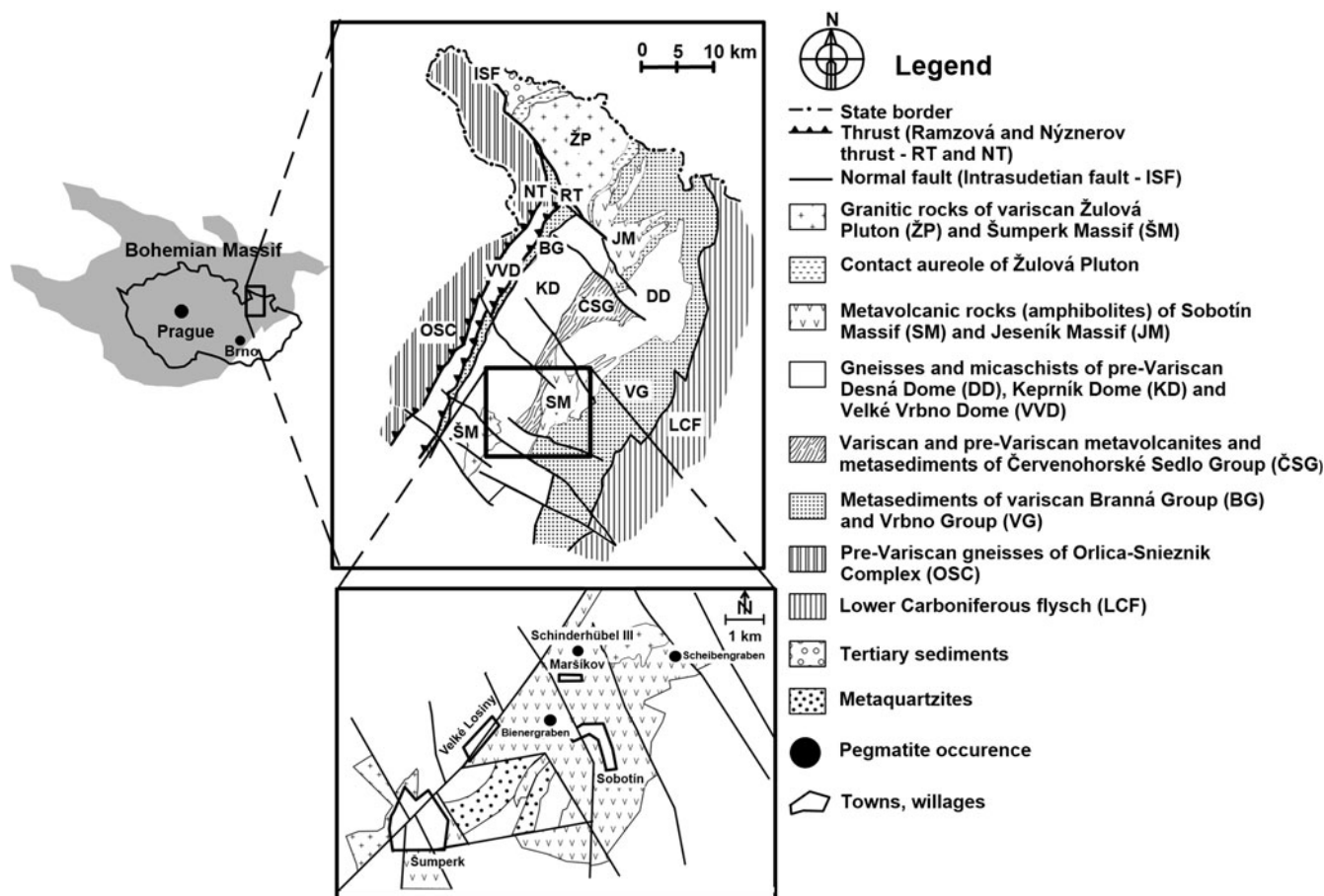


Figure 1. Simplified geological situation of the Maršíkov District with individual pegmatite occurrences (Cháb *et al.*, 2007 and on-line map application of the Czech Geological Survey 2019, Chládek *et al.*, 2020, modified).

The metamorphic rocks of the Desná Dome were intruded primarily in the Maršíkov pegmatite district by numerous dykes or lenticular bodies of granitic pegmatites enclosed in biotite–amphibole gneisses and/or amphibolites of the Sobotín Massif (Fig. 1). The most fractionated pegmatites show an affinity to the LCT (lithium-caesium-tantalum) family and beryl–columbite subtype of the rare-element class according to the classification of Černý and Ercit (2005), as were documented by their mineral assemblages (e.g. Černý *et al.*, 1992, 1995; Novák 1988, 2005; Novák *et al.*, 2003, 2023; Chládek and Zimák, 2016; Chládek *et al.*, 2020, 2021; Dolníček *et al.*, 2020a, 2020b).

The Maršíkov–Schinderhübel III chrysoberyl-bearing granitic pegmatite is situated on the hill NNE of the Maršíkov settlement, a part of Velké Losiny village, ~10 km NE from Šumperk town in the southern part of the Hrubý Jeseník Mountains, northern Moravia region, Czech Republic. It forms a dyke in biotite–hornblende gneiss belonging to Sobotín amphibolite massif. The pegmatite is not exposed, excavation trenches show it to be up to 1 m thickness, with a 160° NNW–SSE strike and inclination of 20° to SW, concordantly to the adjacent gneiss (Dostál, 1966). The pegmatite dyke shows symmetrical internal zoning, including an aplitic unit, an intermediate albite-rich unit with coarse-grained muscovite, and a quartz core unit (Dostál, 1966; Staněk, 1981; Černý *et al.*, 1992; Fig. 2). The aplitic unit is only ~1 cm in thickness and consists of a fine-grained (~0.5 mm) aggregate of albite, quartz, muscovite and garnet (almandine–spessartine) in subordinate amounts, and rare biotite. The intermediate albite-rich unit, ~15–50 cm in thickness, is composed of a medium- to coarse-grained aggregate of albite, quartz and muscovite with abundant fibrolitic sillimanite and relatively common chrysoberyl, garnet, fluorapatite, gahnite, Nb–Ta oxide minerals (columbite- and microlite-group members and fersmite), zircon, uraninite, cheralite, native bismuth and bismutite. Sillimanite, chrysoberyl and muscovite of this unit exhibit a distinct

metamorphic grain lineation parallel to foliation of the pegmatite. The central quartz core unit is ~10 to 40 cm in thickness, and is characterised by less-developed schistosity and contains aggregates of anhedral quartz in association with muscovite, beryl, rare chrysoberyl (more common along the contact of the quartz core with the intermediate unit), sillimanite, garnet, gahnite, and Nb–Ta minerals. The entire Schinderhübel III pegmatite is deficient in K-feldspar (Dostál, 1966; Černý *et al.*, 1992). The other smaller pegmatite dykes with Be minerals (Schinderhübel I and II) occur ~80 m east and ~50 m northwest of the Schinderhübel III pegmatite, and both exhibit similar mineral assemblages with minor to rare K-feldspar and noticeable deformation although accompanied by a lesser degree of metamorphic overprinting and paucity of chrysoberyl and sillimanite (Staněk, 1981; Černý *et al.*, 1992).

Methods

The samples investigated were obtained from several sources, including the Moravian Museum, Brno mineralogical collection and the research collections of Š. Chládek and M. Novák. The abbreviations for the minerals used in the text and figures are after Warr (2021). The composition of minerals were determined on polished sections using a JEOL JXA-8530F field-emission electron-probe microanalyser (EPMA) using wavelength dispersive spectrometry (WDS) at the Institute of the Earth Sciences of the Slovak Academy of Sciences in Banská Bystrica, Slovakia. The following analytical conditions were used: accelerating voltage 15 kV; probe current 20 nA; beam diameter ranging from 3 to 5 µm; and the ZAF matrix correction. The following standards and X-ray lines were used: diopside (SiK α , MgK α , CaK α); rutile (TiK α); albite (AlK α , NaK α); cassiterite (SnL α); ScVO₄ (ScK α , VK α); Cr₂O₃ (CrK α); GaAs (GaL α); YPO₄ (YL α); hematite (FeK α); rhodonite (MnK α); forsterite (MgK α); gahnite

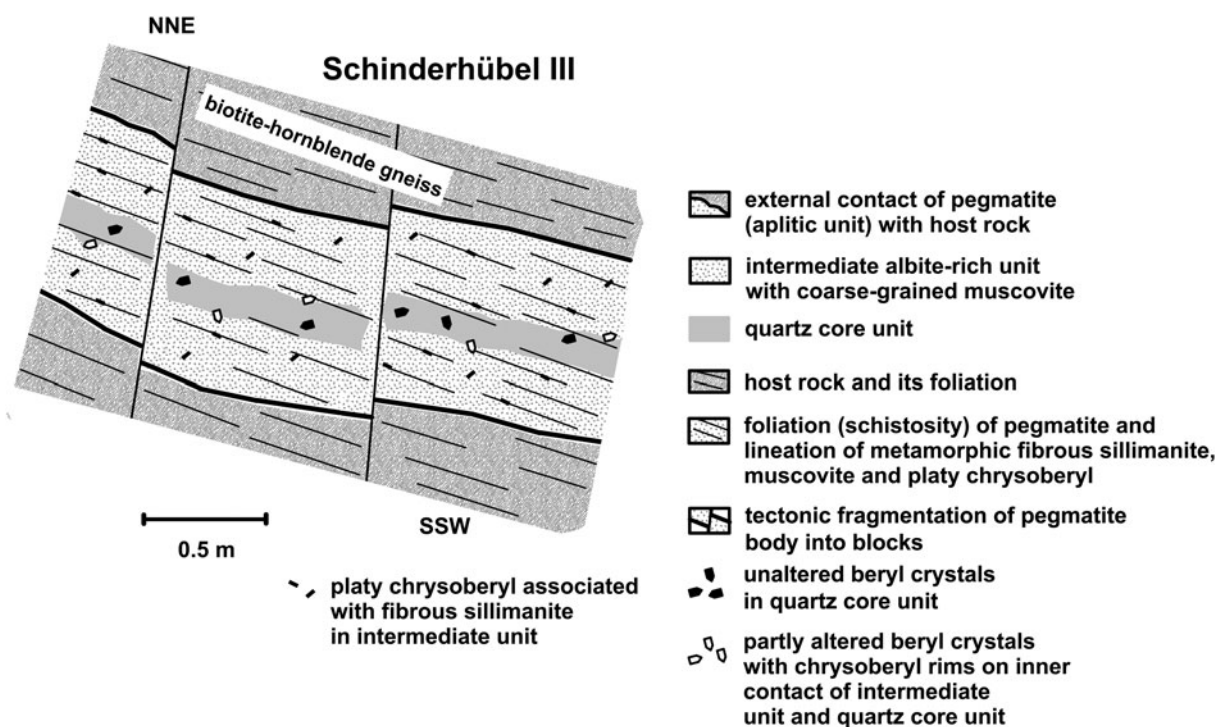


Figure 2. Idealised cross-section of the Maršíkov–Schinderhübel III pegmatite.

(ZnK α); fluorapatite (CaK α); celestine (SrL α); orthoclase (KK α); Rb₂ZnSi₃O₁₂ glass Rb (RbL α); pollucite (CsL α); and fluorite (FK α). Back-scattered electron (BSE) images and X-ray element maps were obtained on the same JEOL JXA-8530F instrument for detailed study of textural relationships among minerals. The element-distribution maps were produced using an accelerating voltage of 15 kV, probe current of 50 nA and 1 μ m beam diameter. The maps comprise 1070 \times 770 pixels, with a pixel size of 0.7 μ m and a dwell time of 50 ms for each pixel.

The trace-element content of chrysoberyl was obtained by laser ablation-inductively coupled plasma-mass spectrometry (LA-ICP-MS) at the Department of Chemistry, Masaryk University, Brno, Czech Republic. The LA-ICP-MS setup consists of the laser ablation system Analyte G2+ (Teledyne Cetac) and the quadrupole ICP-MS Agilent 7900 (Agilent Technologies). The laser ablation system uses a Q-switched Nd-YAG laser-ablation device at the fifth harmonic frequency corresponding to 213 nm wavelength. The ablation cell was flushed with a He carrier gas, which transported the laser-induced aerosol to the inductively coupled plasma (1 l/min). Sample Ar gas flow was admixed with the He gas flow to 1.6 l/min total gas flow. ICP-MS parameters were optimised with respect to maximum signal-to-noise ratio and minimum oxide formation (ThO⁺/Th⁺ count ratio = 0.2%, U⁺/Th⁺ count ratio = 1.1%). The following laser ablation parameters were used for the analysis: 100 μ m laser spot diameter; 8 J cm⁻² laser fluence; and 20 Hz repetition rate. Fixing the sample position during laser ablation facilitated a hole-drilling duration of 60 s for each spot. The NIST SRM 610 silicate glass was used as reference material. All element measurements were normalised to the average concentration of Al in the chrysoberyl, determined by the electron microprobe.

Micro-Raman analyses of minerals were performed on the LabRAM-HR Evolution Horiba Jobin-Yvon spectrometer system with a Peltier-cooled CCD detector and Olympus BX-41 microscope (Department of Geological Sciences, Masaryk University, Brno, Czech Republic). Raman spectra were excited by a blue diode laser (473 nm) with a power of 2.5 mW in the range of 100–4,000 cm⁻¹ and 100–10,000 cm⁻¹ were collected from each mineral using a 50 \times objective. The acquisition time of 30 s and 5 s per frame, respectively, and two accumulations were used to improve the signal-to-noise ratio. Raman spectra were also obtained using a Thermo Scientific DXR3xi Raman imaging microscope at the Natural History Museum in Bratislava, Slovakia. The doubled Nd: YVO₄ DPSS excitation laser (532 nm) and He-Ne laser (633 nm), 100 \times objective, a 25 μ m confocal pinhole, and an EMCCD detector were used. The spectra were acquired at a laser power of 10–20 mW and 0.5–2 s (20 scans for a cycle), and they were processed in the Seasolve *PeakFit 4.1.12* software. Raman bands were fitted by the Lorentz function with automatic background correction and Savitzky-Golay smoothing.

Powder X-ray diffraction (XRD) analysis was determined by the BRUKER D8 Advance diffractometer (Department of Mineralogy and Petrology, Comenius University, Bratislava) under the following conditions: Bragg-Brentano geometry (θ –2 θ), Cu anticathode (K α ₁ = 1.5406 Å), accelerating voltage = 40 kV and beam current = 40 mA; a NiK β filter was used for stripping K β radiation, and data were obtained by a BRUKER LynxEye detector. The step size was 0.01 $^\circ$ 2 θ with a counting time of 5 s per step, and 2 θ measurement ranged from 4 to 65 $^\circ$. The lattice parameters were refined with the Bruker DIFFRAC plus TOPAS software using the structural model for chrysoberyl (Hazen and Finger, 1987).

Results

Textural and paragenetic relationships of Be minerals

The following Be minerals were identified in the pegmatite: chrysoberyl; beryl; euclase; and bertrandite. Chrysoberyl occurs in intermediate and quartz core units as transparent to translucent subhedral to anhedral rarely euhedral prismatic to tabular crystals and V-shaped twins (~50 μ m to 3 cm in size) with yellow-green to pale-green colour and vitreous to adamantine lustre. Chrysoberyl is associated with beryl, quartz, albite, muscovite and sillimanite in the intermediate unit or in its contact with the quartz core. In the outer parts of the intermediate unit, platy crystals of chrysoberyl are commonly parallel to flakes of muscovite and fibrolitic sillimanite aggregates and relics of primary beryl are absent or very rare. The BSE images of chrysoberyl exhibit mostly patchy, rarely irregular lamellar or concentric zonation of crystals (Figs 3,4,5), some large platy chrysoberyl crystals without relics of beryl show fine lamellar to oscillatory growth zoning (Fig. 3e,f). Relics of primary beryl and inclusions of quartz, albite, muscovite, gahnite, and Nb–Ta oxide minerals are commonly detected in chrysoberyl (Figs 3,4,5). Secondary Fe-rich beryl, euclase, bertrandite and late muscovite are locally confined to the edges and fractures of chrysoberyl (Figs 4b,e, 5).

Primary beryl occurs as euhedral to subhedral pale yellow-green or bluish green translucent prismatic crystals, up to 5 cm in length and 2 cm in thickness, typically in the quartz core. In the intermediate unit, crystals of primary beryl are replaced by chrysoberyl, and locally, anhedral relicts of beryl (20–300 μ m across) are associated with quartz at inner contact of the intermediate unit and quartz core units (Figs 3a,b,d, 5). Larger subhedral crystals of beryl (~200 to 500 μ m) also occur with chrysoberyl and albite (Fig. 4c).

Anhedral domains of secondary Fe-rich beryl, ~50 μ m large, were rarely identified in rims of chrysoberyl crystals (Fig. 5a–d). Euclase forms subhedral to anhedral overgrowths and veinlets replacing chrysoberyl, usually ~50 μ m to 1 mm in size (Figs 3a, 4b,e, 5). Bertrandite occurs as anhedral grains or veinlets, up to 200 μ m in size, located in chrysoberyl, and locally replaces euclase (Fig. 4b).

Composition of Be minerals

The zoning in BSE images (Figs 3–5) generally reflects different Fe concentrations in chrysoberyl with the lighter zones illustrating domains with elevated contents of Fe in chrysoberyl (Table 1). Valence calculations indicate the dominance of trivalent Fe in chrysoberyl (1.1–5.3 wt.% Fe₂O₃; \leq 0.09 atoms per formula unit Fe³⁺), however commonly a small amount of Fe²⁺ (\leq 0.5 wt.% FeO) is also present, which correlates positively with Ti (\leq 0.6 wt.% TiO₂; \leq 0.01 apfu) and Sn (\leq 0.5 wt.% SnO₂; \leq 0.004 apfu). Compositional relationships suggest two main octahedral-site substitutions in chrysoberyl: (1) dominant Fe³⁺ = Al³⁺; and (2) minor Fe²⁺ + Ti⁴⁺ = 2(Al,Fe)³⁺ substitutions (Fig. 6).

The LA-ICP-MS investigation of chrysoberyl yielded elevated concentrations of Ga (~240–420 ppm), Sn (~40–440 ppm) and V (~20–180 ppm) together with Fe and Ti (Supplementary Table S1); Cr is frequently below the detection limit. Extraordinarily high concentrations of Ta (\leq 7200 ppm) and Nb (\leq 2700 ppm) were detected locally in chrysoberyl, and they can be explained by micro- to nano-inclusions of Nb–Ta oxide minerals as documented in BSE images (Figs 3a, 4d–f, 5). Positive correlations were observed between some trace elements in chrysoberyl: Sn versus Ti, Hf vs. Zr, V vs. Ti, V vs. Ga and Ti vs. Ta (Fig. 7a–e).

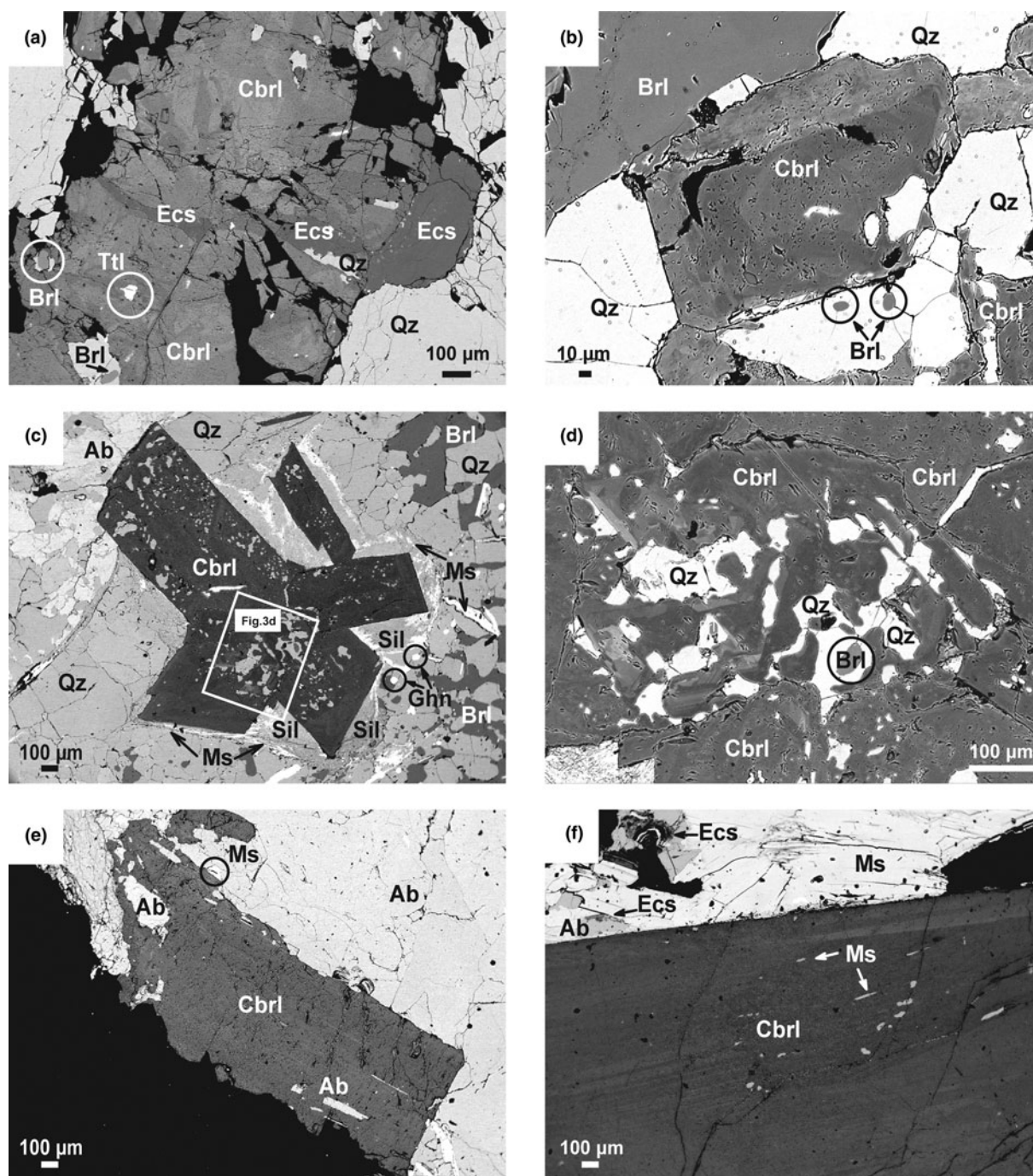


Figure 3. BSE images of chrysoberyl and associated minerals of the Maršíkov–Schinderhübel III pegmatite. Mineral abbreviations: Cbri (chrysoberyl), Bri (primary beryl), Ecs (euclase), Qz (quartz), Ab (albite), Ms (muscovite), Sil (sillimanite), Ttl (Nb–Ta oxide minerals: tantalite, columbite and ixiolite), Gnn (gahnite).

Primary beryl is characterised by a low content of Fe: up to 1.2 wt.% Fe_2O_3 (≤ 0.08 apfu Fe^{3+}) and up to 0.5 wt.% FeO (≤ 0.04 apfu Fe^{2+}). Rare secondary Fe-rich beryl contains 0.7–1.1 wt.% Fe_2O_3 (0.05–0.08 apfu Fe^{3+}), although it is distinctly enriched in FeO (3.1–3.4 wt.%; 0.24–0.27 apfu Fe^{2+}) (Fig. 5d; Table 2). Divalent Fe is compensated by Na (up to 1.6 wt.% Na_2O ; ≤ 0.29 apfu Na) according to the channel (C) – octahedral (O) substitution: ${}^{\text{C}}\text{Na}^+ + {}^{\text{O}}\text{M}(\text{Fe}, \text{Mn}, \text{Mg}, \text{Zn})^{2+} = {}^{\text{C}}\square + {}^{\text{O}}\text{Al}^{3+}$, and Fe^{3+} replaces Al in octahedral, stoppaniite-type substitution: ${}^{\text{C}}\text{Fe}^{3+} = {}^{\text{C}}\text{Al}^{3+}$ (Fig. 8). The concentrations of other elements are negligible except for 0.2 wt.% MnO (0.02 apfu Mn) in Fe-rich beryl (Table 2).

Euclase contains up to 0.4 wt.% Fe_2O_3 (0.01 apfu Fe) and negligible amounts of Zn and Ca (≤ 0.1 oxide wt.%) (Table 3). Bertrandite is also close to the end-member composition (Table 4).

Unit-cell parameters and Raman spectroscopy of the Be minerals

The unit-cell parameters of the chrysoberyl determined by powder X-ray diffraction (Table 5) are in excellent accordance with the previously published data (Dostál, 1969; Hazen and Finger, 1987). The presence of bertrandite was also confirmed by micro-Raman spectroscopy as EPMA cannot distinguish

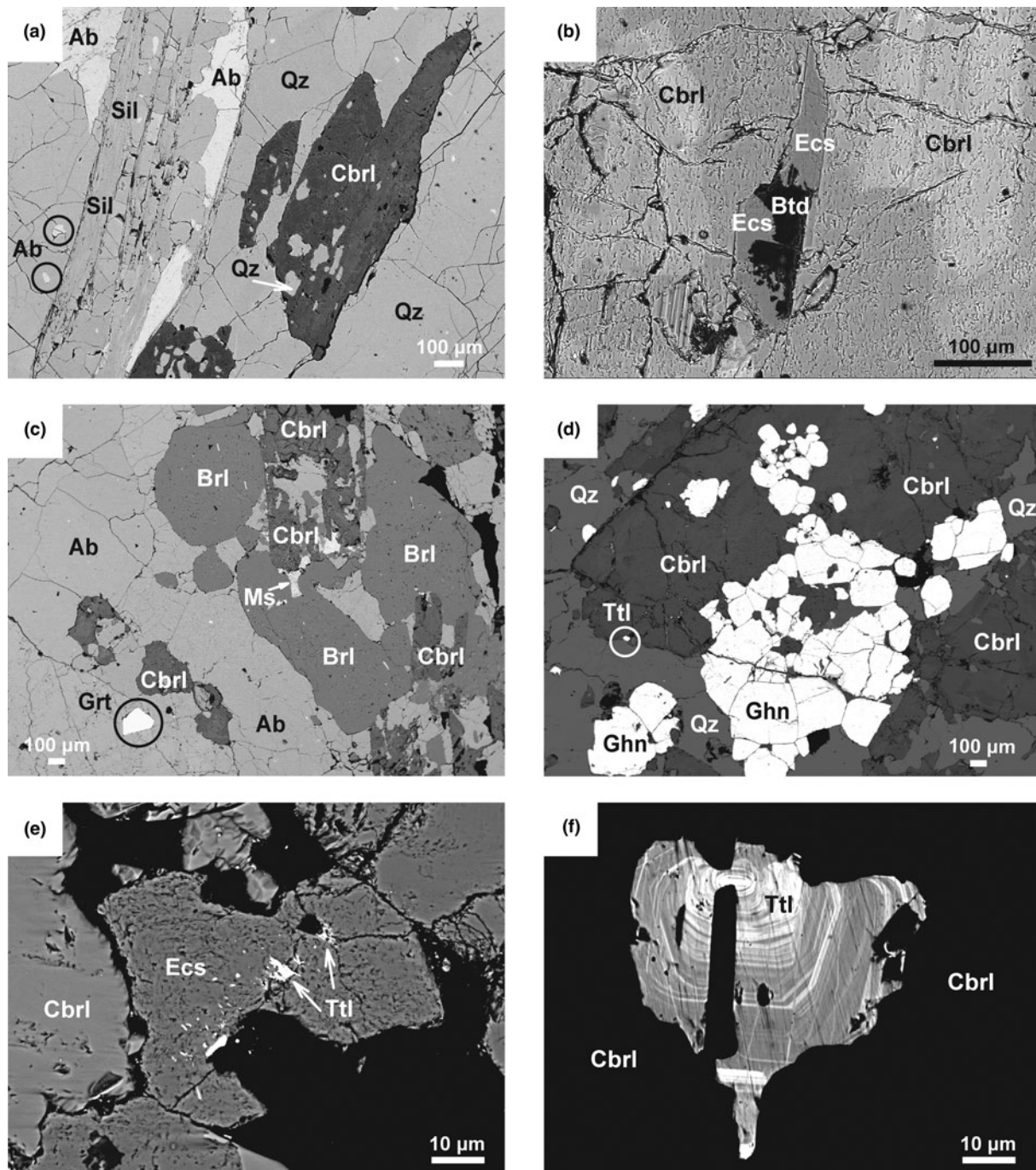


Figure 4. BSE images of chrysoberyl and associated minerals of the Maršíkov–Schinderhübel III pegmatite. Mineral abbreviations as in Fig. 3, Btd (bertrandite), Grt (garnet).

bertrandite from phenakite. The Raman spectra of bertrandite from the Maršíkov–Schinderhübel III pegmatite (Fig. 9) are in excellent agreement with the RRUFF database (R060803.3 and R050032.3 samples; Lafuente *et al.*, 2016). Note that the bertrandite spectrum also shows some typical bands for closely-associated euclase.

Discussion

Chrysoberyl composition

Several studies have focused on the description of minerals and geology from the Maršíkov–Schinderhübel III pegmatite (e.g.

Kretschmer, 1911; Dostál, 1966, 1969; Černý *et al.*, 1992); however, a detailed study of the textural relations and compositional variations in chrysoberyl and its mineral assemblage is lacking. The composition of natural chrysoberyl is typically close to the BeAl_2O_4 end-member formula. The olivine-type structure of chrysoberyl is composed of two principal cation sites: octahedrally coordinated $M1$ and $M2$ sites are occupied by Al^{3+} , and the tetrahedral (T) position is filled by Be^{2+} cations (Hawthorne and Huminicki, 2002). Aluminium in the octahedral sites is commonly replaced by other trivalent cations, especially by Cr^{3+} and Fe^{3+} . The maximum Fe_2O_3 content reported in natural chrysoberyl is 6.25 wt.% for samples from the Kalanga Hill

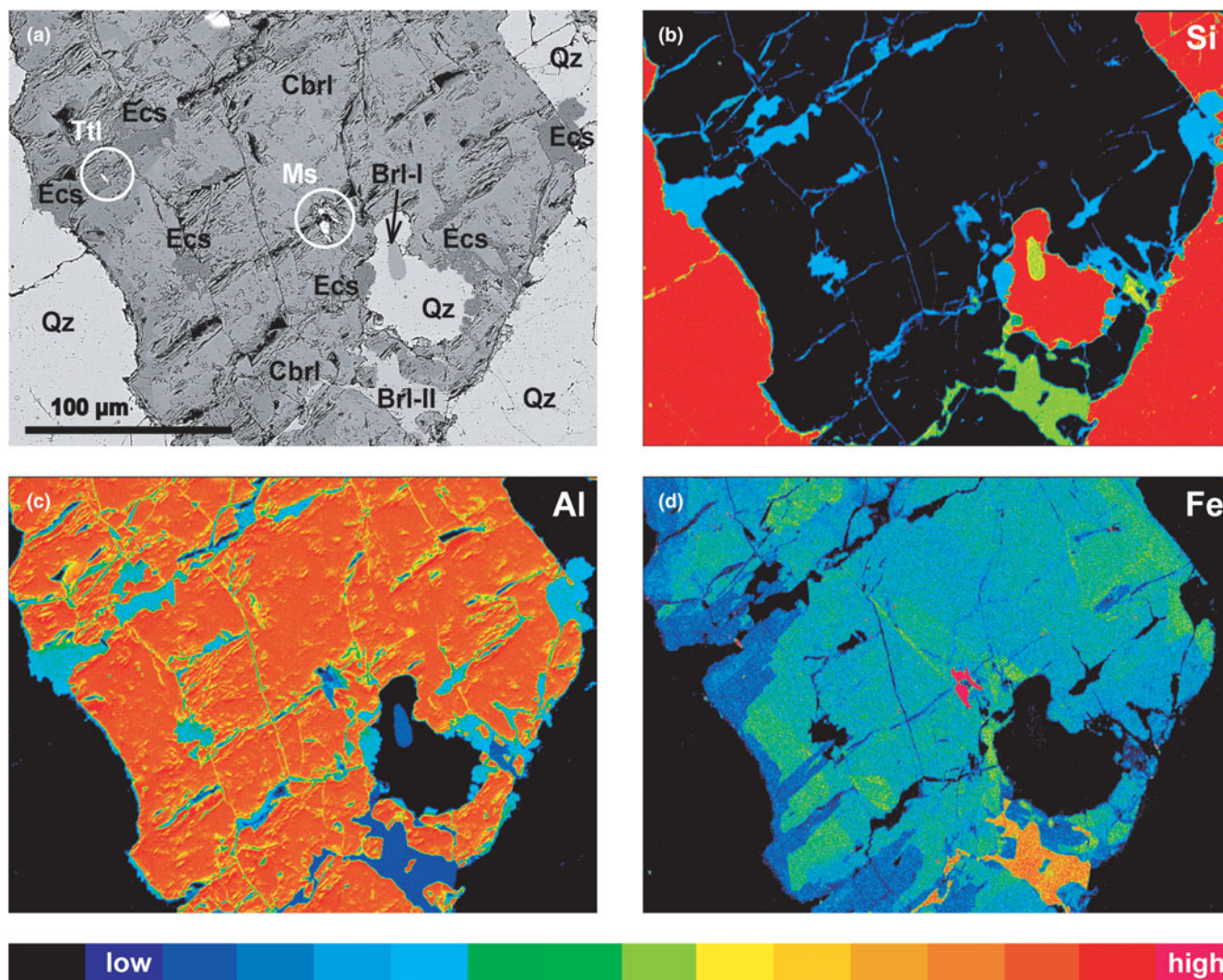


Figure 5. BSE image: (a) and element-distribution maps of Si, Al and Fe; (b–d) of chrysoberyl from the Maršíkov–Schinderhübel III pegmatite. Chrysoberyl contains tantalite inclusion, remnants of primary beryl (Brl-I), and secondary Fe-rich beryl (Brl-II), secondary muscovite and euclase. Mineral abbreviations as in Fig. 3.

pegmatite, Zambia (Žáček and Vrána, 2002). Chrysoberyl from the Maršíkov–Schinderhübel III pegmatite exhibits relatively broad variations of Fe (1.1 to 5.3 wt.% Fe_2O_3 and ≤ 0.5 wt.% FeO). Elevated Fe contents are typical of chrysoberyl of metamorphic origin, whereas magmatic chrysoberyl from leucogranites and pegmatites usually have a lower Fe content (≤ 1.2 wt.% FeO total; Merino *et al.*, 2013).

Contents of Ti (≤ 0.6 wt.% TiO_2 ; ≤ 0.01 apfu), Ga (~240–420 ppm), Sn (~40–440 ppm), and V (~20–180 ppm) in the Maršíkov chrysoberyl are comparable with the published data (≤ 0.7 wt.% TiO_2 , ≤ 4500 ppm Sn, ≤ 1600 ppm Ga and 1200 ppm V; Soman and Nair, 1985; Merino *et al.*, 2013; Kanouo *et al.*, 2016; Schmetzer *et al.*, 2016; Sun *et al.*, 2019; Colombo *et al.*, 2021). High concentrations of Ta (up to ~7200 ppm) and Nb (up to ~2700 ppm), detected in the Maršíkov chrysoberyl, are very unusual and probably result from the presence of numerous nano- to micro-inclusions of Nb–Ta oxide minerals (columbite-(Fe), columbite-(Mn), tantalite-(Fe), tapiolite-(Fe), ixiolite-(Mn^{2+}); Figs 3–5). Such high contents of Ta and Nb have not been found previously in chrysoberyl; ~510 ppm Ta and ~250 ppm Nb are

the maximum reported (Merino *et al.*, 2013; Kanouo *et al.*, 2016; Schmetzer *et al.*, 2016; Colombo *et al.*, 2021).

Evolution of the chrysoberyl assemblage

The origin of chrysoberyl in granitic pegmatites can be explained by two principal hypotheses: either primary magmatic or metamorphic genesis. The main criteria for distinguishing between these hypotheses are textural relationships, mineral paragenesis and the presence or absence of metamorphic overprint in the parental pegmatite. Moreover, Fe content in chrysoberyl can also be an indicator of magmatic *versus* metamorphic origin (Merino *et al.*, 2013).

Schistosity and fragmentation of the pegmatite body into blocks as a result of superimposed stress, mineral lineation and presence of fine-crystalline bands of fibrolitic sillimanite parallel to the host gneiss foliation, and replacement of beryl by chrysoberyl are distinct features of metamorphic overprinting of the Maršíkov–Schinderhübel III pegmatite (Dostál, 1966, 1969;

Table 1. Representative compositions (wt.%) and formulae (apfu) of chrysoberyl from the Maršíkov pegmatite.

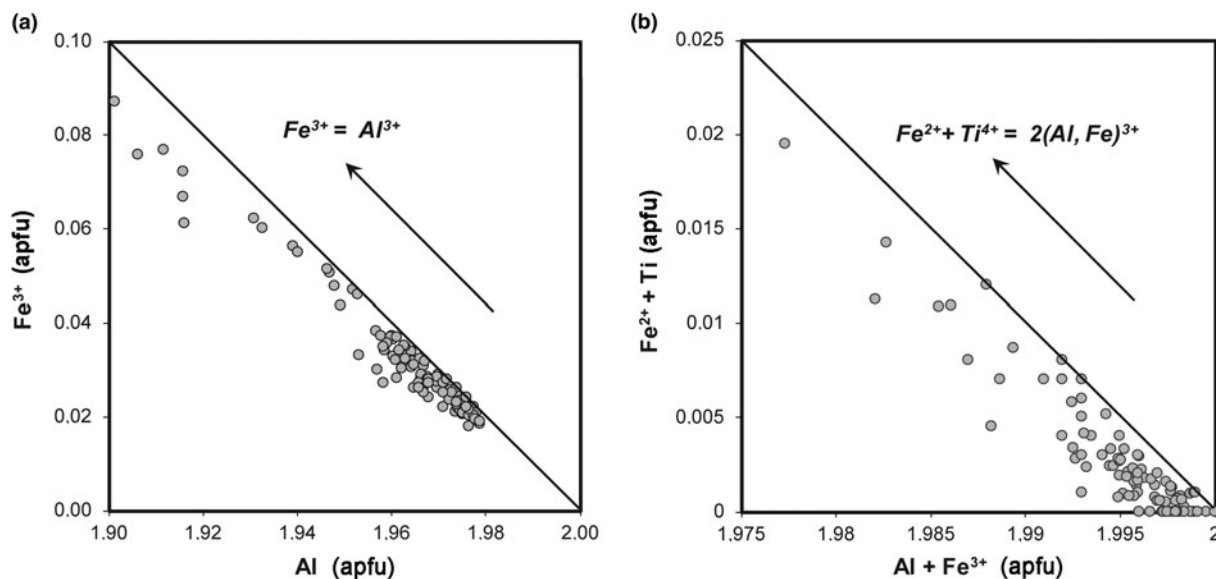
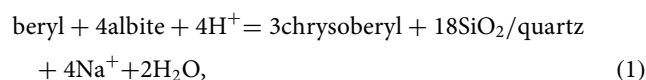
Analyse #	SCH-8-1	SCH-8-3	SCH-8-4	SCH-8-5	SCH-1C-2	SCH-1C-7	SCH-2-1	SCH-2-2
SiO ₂	bdl	bdl	bdl	0.07	bdl	bdl	bdl	bdl
TiO ₂	bdl	0.08	0.62	0.18	0.11	0.08	0.10	0.12
SnO ₂	bdl	0.06	0.22	0.47	0.06	0.05	bdl	bdl
Al ₂ O ₃	77.47	77.00	75.93	73.92	77.97	77.35	78.48	78.45
Sc ₂ O ₃	0.03	bdl	bdl	bdl	0.06	bdl	0.03	bdl
V ₂ O ₃	bdl	bdl	0.04	0.07	0.05	bdl	bdl	bdl
Ga ₂ O ₃	bdl	0.07	bdl	bdl	bdl	0.12	0.08	0.04
Fe ₂ O ₃	1.98	2.96	3.79	5.29	1.69	2.36	1.27	1.11
FeO	bdl	0.06	0.53	0.09	0.13	0.04	bdl	0.07
BeO (calculated)	19.32	19.39	19.43	19.05	19.45	19.39	19.49	19.47
Total	98.80	99.62	100.56	99.14	99.52	99.39	99.45	99.26
Mineral formulae based on 4 oxygen atoms, 1 Be atom, 3(T + O atoms) and valence calculation								
Si				0.001				
Be	1.000	1.000	1.000	1.000	1.000	1.000	1.000	1.000
Sum T	1.000	1.000	1.000	1.001	1.000	1.000	1.000	1.000
Ti		0.001	0.010	0.003	0.002	0.001	0.002	0.002
Sn		0.001	0.002	0.004	0.000	0.000		
Al	1.967	1.948	1.917	1.903	1.967	1.958	1.976	1.978
Sc	0.001				0.001		0.001	
V			0.001	0.001	0.001			
Ga		0.001				0.002	0.001	0.001
Fe ³⁺	0.032	0.048	0.061	0.087	0.027	0.038	0.020	0.018
Fe ²⁺		0.001	0.009	0.002	0.002	0.001		0.001
Sum O	2.000	2.000	2.000	2.000	2.000	2.000	2.000	2.000
Al ₂ BeO ₄ (mol.%)	98.4	97.6	96.9	95.6	98.6	98.1	99.0	99.1
Fe ₂ ³⁺ BeO ₄ (mol.%)	1.6	2.4	3.1	4.4	1.4	1.9	1.0	0.9

bdl – below detection limit

Staněk 1981; Franz and Morteani, 1984; Černý *et al.*, 1992). The metamorphic overprinting also caused partial dissolution–reprecipitation of accessory columbite–tantanite with extensive compositional and structural re-equilibration and homogenisation of primary magmatic Nb–Ta oxide minerals (Černý *et al.*, 1992). Our observations corroborate metamorphic crystallisation of chrysoberyl by a breakdown of primary magmatic beryl, together with the coeval formation of metamorphic fibrolitic sillimanite, quartz and muscovite (Figs 3c, 4a). Detailed inspection of microtextures revealed the presence of small, commonly oval, relicts of

primary beryl in chrysoberyl or in quartz (Figs 3a,b,d, 5a) or growth of chrysoberyl crystals at the expense of primary magmatic beryl (Fig. 4c).

The following reactions have been suggested for the formation of new metamorphic assemblages from a primary magmatic beryl and associated minerals (Franz and Morteani, 1984, 2002):

**Figure 6.** Substitution diagrams of chrysoberyl from the Maršíkov–Schinderhübel III pegmatite: (a) Fe³⁺ = Al³⁺; (b) Fe²⁺ + Ti⁴⁺ = 2(Al, Fe)³⁺.

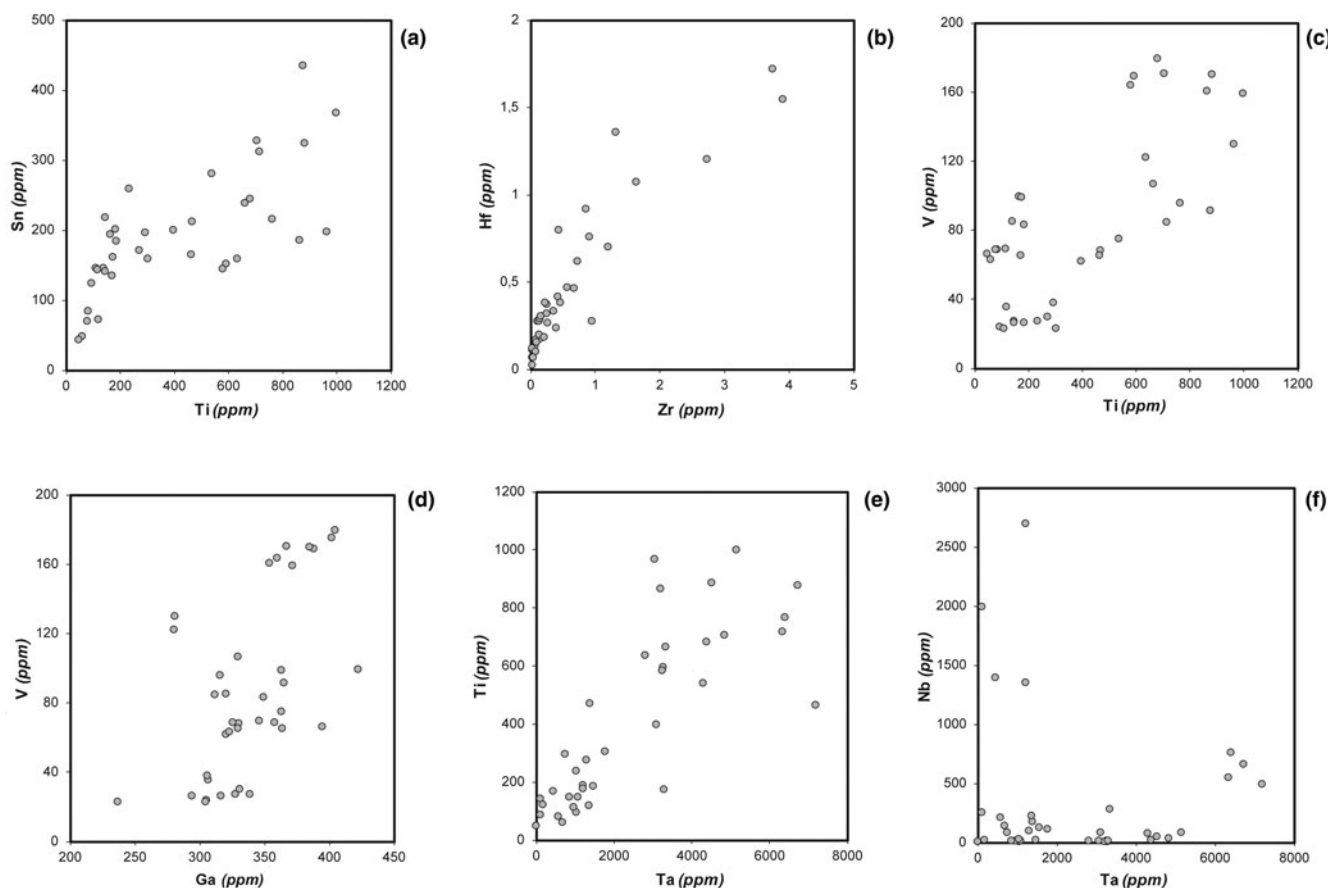
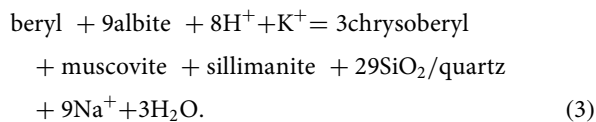
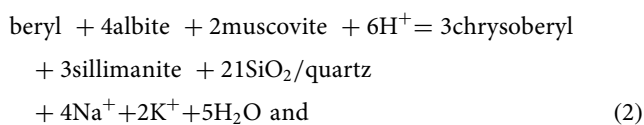
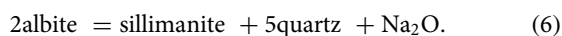
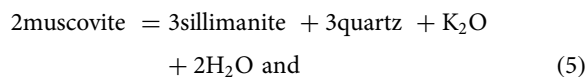
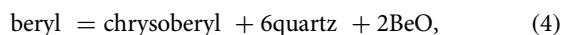


Figure 7. Correlation diagrams of trace elements from the Maršíkov-Schinderhübel III pegmatite (in ppm): (a) Sn vs. Ti; (b) Hf vs. Zr; (c) V vs. Ti; (d) V vs. Ga; (e) Ti vs. Ta; (f) Nb vs. Ta.



Černý *et al.* (1992) have also proposed the following reactions:



The assemblage chrysoberyl + quartz \pm fibrolitic sillimanite \pm muscovite might be explained by the reactions 1 to 4. Aggregates of fibrolitic sillimanite (\pm tiny metamorphic muscovite) form

overgrowths on chrysoberyl crystals, or they occur in close vicinity (Figs 3c, 4a). Reaction 4 suggests that part of the Be from primary magmatic beryl escaped into fluids which might have facilitated precipitation of a distal chrysoberyl without close contact with primary magmatic beryl (Fig. 3e,f).

Experimental data and the presence of sillimanite clearly indicate high-temperature conditions for the beryl breakdown to a chrysoberyl and quartz assemblage, generally over 500–600°C (Franz and Morteani, 1984, 2002; Barton 1986; Barton and Young, 2002, and references therein). Černý *et al.* (1992) estimated temperatures of 570–630°C and pressures of 250–500 MPa for the metamorphic formation of chrysoberyl in the Maršíkov-Schinderhübel III pegmatite. Variscan prograde medium- to high-temperature metamorphism at $T \approx 540\text{--}660^\circ\text{C}$ and $P \approx 500\text{--}700$ MPa (Souček, 1978; René, 1983; Cháb *et al.*, 1990; Schulmann and Gayer, 2000; Košuličová and Štípská, 2007; Schulmann *et al.*, 2014) is probably responsible for the origin of metamorphic chrysoberyl and sillimanite in the Maršíkov-Schinderhübel III pegmatite. However, our textural and paragenetic observations do not support dividing the prograde metamorphic overprinting of the Maršíkov-Schinderhübel III pegmatite into two stages as Černý *et al.* (1992) proposed as an explanation for what appeared to be two generations of chrysoberyl. Chrysoberyl has also been found at several granitic pegmatites in the northern region around Česká Ves where it is commonly associated with rare sillimanite (e.g. Novák and Rejl, 1993). Hence, the metamorphic assemblage chrysoberyl + sillimanite in granitic pegmatites shows a regional

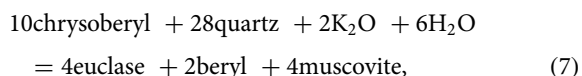
Table 2. Representative compositions (wt.%) and mineral formulae (apfu) of beryl from the Maršikov pegmatite.

Sample #	SCH-7-14	SCH-1E-10	SCH-8-6	SCH-4-8	SCH-4-9	SCH-4-10
Type	Primary Fe-poor beryl			Secondary Fe-rich beryl		
SiO ₂	65.27	65.62	65.63	63.24	62.91	63.39
TiO ₂	bdl	bdl	bdl	0.04	0.04	0.05
Al ₂ O ₃	18.26	18.23	18.23	14.63	14.69	14.85
V ₂ O ₃	0.09	bdl	bdl	bdl	bdl	bdl
Fe ₂ O ₃	0.09	0.67	1.19	1.14	0.68	0.83
FeO	0.46	0.21	bdl	3.06	3.41	3.17
MnO	bdl	0.07	bdl	0.22	0.17	0.20
ZnO	0.04	bdl	0.08	0.07	0.04	0.03
MgO	bdl	bdl	bdl	0.04	0.03	0.03
CaO	0.10	bdl	bdl	bdl	bdl	bdl
SrO	0.09	0.04	bdl	0.04	bdl	bdl
BeO (calc.)	13.63	13.71	13.75	13.15	13.09	13.18
Na ₂ O	0.16	0.23	0.15	1.40	1.55	1.44
Cs ₂ O	0.06	bdl	0.04	bdl	bdl	bdl
Total	98.25	98.78	99.07	97.03	96.61	97.17
Mineral formulae based on 18 O and 3 Be atoms, 8(Tl + O) cations and valence calculation						
Si	5.978	5.976	5.965	6.006	6.003	6.005
Al Tl	0.022	0.024	0.035	0.000	0.000	0.000
Sum Tl	6.000	6.000	6.000	6.006	6.003	6.005
Ti				0.003	0.003	0.004
Al O	1.949	1.933	1.918	1.638	1.652	1.658
V	0.007					
Fe ³⁺	0.006	0.046	0.081	0.082	0.049	0.059
Fe ²⁺	0.035	0.016		0.243	0.272	0.251
Mn	0.000	0.005		0.018	0.014	0.016
Zn	0.003	0.000	0.005	0.005	0.003	0.002
Mg				0.006	0.004	0.004
Sum O	2.000	2.000	2.004	1.995	1.997	1.994
Be T2	3.000	3.000	3.000	3.000	3.000	3.000
Ca	0.010					
Sr	0.005	0.002		0.002		
Na	0.028	0.041	0.026	0.258	0.287	0.265
Cs	0.002		0.002			
Sum C	0.045	0.043	0.028	0.260	0.287	0.265
Al total	1.971	1.957	1.953	1.638	1.652	1.658
Sum cations	11.045	11.043	11.032	11.261	11.287	11.264

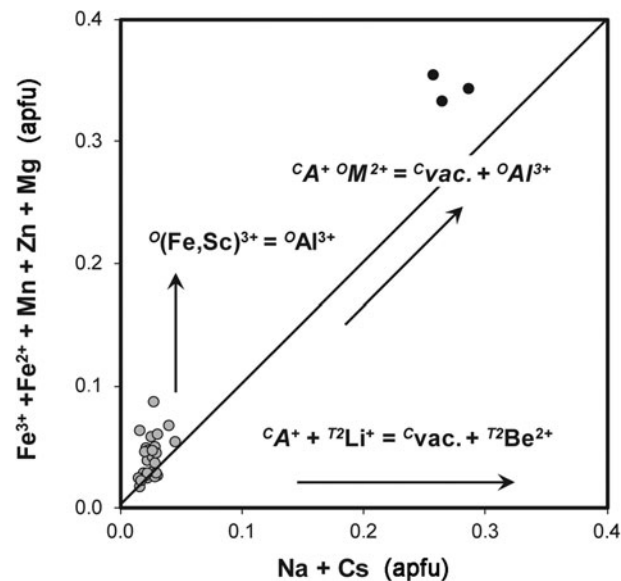
bdl – below detection limit. Other elements not listed: Cr, Ga, Sc, Y, K and Rb are also below the detection limit.

distribution generally consistent with a single Variscan prograde metamorphism in the examined region.

Investigation of mineral textures and composition also indicates a retrograde metamorphic stage in the Maršikov-Schinderhübel III pegmatite. Chrysoberyl is replaced locally by secondary Fe-rich beryl, euclase, and late muscovite along veinlets and irregular rim domains (Figs 3a, 4b,e, 5). The textural relationships support partial replacement of euclase by bertrandite, whereas adjacent chrysoberyl is intact (Fig. 4b). For this retrograde stage, the following reactions are proposed:



Experimental studies indicate a lower stability of beryl at ~300–400°C, whereas euclase is stable at ~300–450°C, and bertrandite below 250°C at a pressure up to 300 MPa (Franz and

**Figure 8.** Substitution $\text{Fe}^{3+} + \text{Fe}^{2+} + \text{Mn} + \text{Zn} + \text{Mg}$ vs. $\text{Na} + \text{Cs}$ diagram of beryl from the Maršikov-Schinderhübel III pegmatite. Notes: primary magmatic beryl (grey circles), secondary Fe-rich beryl (black circles).**Table 3.** Representative (wt.%) and mineral formulae (apfu) of euclase from Maršikov pegmatite.

Sample #	SCH-1b-6	SCH-1b-7	SCH-1e-3	SCH-1e-9	SCH-2-12
SiO ₂	41.18	40.98	40.42	39.88	41.51
Al ₂ O ₃	34.63	34.40	34.32	34.20	34.17
V ₂ O ₃	bdl	bdl	bdl	0.05	bdl
Ga ₂ O ₃	0.04	bdl	bdl	bdl	bdl
Fe ₂ O ₃	0.08	0.06	0.10	0.09	0.43
MnO	bdl	0.03	0.07	0.03	bdl
ZnO	0.09	0.03	0.07	0.11	bdl
BeO (calc.)	17.16	17.01	16.91	16.75	17.14
MgO	bdl	bdl	bdl	bdl	0.02
CaO	0.02	0.02	0.07	0.05	0.10
Na ₂ O	0.09	bdl	bdl	bdl	bdl
K ₂ O	0.02	bdl	bdl	bdl	0.07
H ₂ O (calc.)	6.18	6.11	6.09	6.00	6.17
F	bdl	0.03	bdl	0.08	bdl
Total	99.51	98.67	98.05	97.23	99.61
Mineral formulae based on 5 anions, 1(OH+F) and 1 Be atom					
Si	0.999	1.003	0.995	0.991	1.008
Al	0.001	0.000	0.005	0.009	0.000
Sum T	1.000	1.003	1.000	1.000	1.008
Al	0.989	0.992	0.991	0.992	0.978
V				0.001	
Ga	0.001				
Fe	0.002	0.001	0.002	0.002	0.008
Mn		0.001	0.001	0.001	
Mg					0.001
Zn	0.002	0.001	0.001	0.002	
Sum O	0.993	0.995	0.996	0.998	0.987
Be	1.000	1.000	1.000	1.000	1.000
Ca	0.001	0.001	0.002	0.001	0.003
Na	0.004				
K	0.001				0.002
Sum A	0.005	0.001	0.002	0.001	0.005
OH	1.000	0.998	1.000	0.994	1.000
F		0.002		0.006	
Sum X	1.000	1.000	1.000	1.000	1.000

bdl – below detection limit. Other elements not listed: Ti, Sn, Cr, Sc, Y, Ni, Mg, Sr, Rb, Cs and Cl are also below the detection limit.

Table 4. Representative (wt.%) and mineral formulae (apfu) of bertrandite from the Maršíkov pegmatite.

Sample	SCH-1-11	SCH-1e-4	SCH-3-18	SCH-3-19
SiO ₂	48.34	49.60	49.56	49.69
TiO ₂	bdl	0.03	0.04	bdl
Al ₂ O ₃	1.56	0.14	0.28	0.09
Ga ₂ O ₃	0.09	0.02	0.05	bdl
Cr ₂ O ₃	0.06	bdl	0.02	bdl
V ₂ O ₃	bdl	0.02	bdl	bdl
Sc ₂ O ₃	bdl	0.02	bdl	bdl
Fe ₂ O ₃	0.03	0.06	0.07	bdl
ZnO	bdl	0.04	0.05	0.08
BeO (calc.)	41.92	41.56	41.69	41.54
CaO	0.06	bdl	bdl	bdl
SrO	0.03	0.04	bdl	bdl
Na ₂ O	0.13	0.01	0.01	0.02
K ₂ O	0.07	0.01	0.08	0.04
H ₂ O (calc.)	7.55	7.47	7.51	7.47
F	bdl	0.02	bdl	0.01
Total	99.83	99.05	99.35	98.94
Mineral formulae based on 9 anions, 2B cations, 4 Be atoms and 2(OH+F)				
Si	1.920	1.988	1.980	1.992
Ti		0.001	0.001	
Al	0.073	0.007	0.013	0.004
Ga	0.002	0.001	0.001	
Cr	0.002		0.001	
V		0.001		
Sc		0.001		
Fe	0.001	0.002	0.002	
Zn		0.001	0.002	0.002
Sum B	2.000	2.000	2.000	2.000
Be	4.000	4.000	4.000	4.000
Ca	0.002			
Sr	0.001	0.001		
Na	0.010	0.001	0.001	0.001
K	0.004	0.001	0.004	0.002
Sum A	0.017	0.003	0.005	0.003
OH	2.000	1.997	2.000	2.000
F		0.003		0.000
Sum X	2.000	2.000	2.000	2.000

bdl – below detection limit. Other elements not listed: Sn, Mn, Ni, Mg, Rb, Cs and Cl are also below the detection limit.

Table 5. The unit-cell parameters of chrysoberyl from the Maršíkov pegmatite calculated from powder XRD and compared with published data.

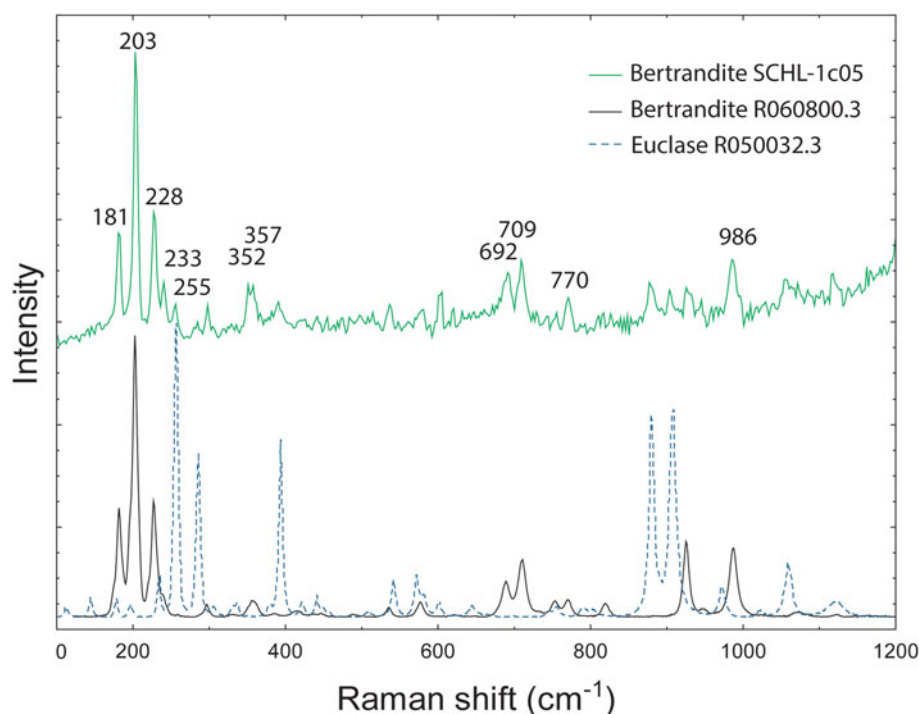
Locality/Reference	<i>a</i> (Å)	<i>b</i> (Å)	<i>c</i> (Å)	<i>V</i> (Å ³)
Maršíkov (this study)	4.4289(8)	9.413(2)	5.480(1)	228.457
Maršíkov (Dostál, 1969)	4.430(2)	9.414(8)	5.477(4)	228.413
Hazen and Finger (1987)	4.424(1)	9.396(1)	5.471(2)	227.5(1)

Morteani 1981, 2002; Barton 1986; Barton and Young, 2002; Grew, 2002, and reference therein). However, a recent study of secondary Be minerals and their mineral assemblages from granitic pegmatites (Novák *et al.*, 2023) suggests the stability of bertrandite up to $T \approx 300^\circ\text{C}$. Consequently, this late retrograde metamorphic event occurred at $T \approx 500$ to 200°C and $P \leq 250$ MPa. The existence of the Permian post-Variscan thermal overprinting (~ 280 to 260 Ma) is documented in the Hrubý Jeseník Mountains by K–Ar mica and U–Th–Pb monazite radiometric age determinations; the event was probably associated with renewed fluid activity along the Sudetic fault system (Schulmann *et al.*, 2014).

Conclusions

A study of the compositional variation of chrysoberyl indicates the following principal substitution mechanisms in the octahedral sites: (1) $\text{Fe}^{3+} = \text{Al}^{3+}$ and (2) $\text{Fe}^{2+} + \text{Ti}^{4+} = 2(\text{Al}, \text{Fe})^{3+}$. Moreover, the characteristic trace elements incorporated in the chrysoberyl structure are Ga, Sn and V, whereas unusually high Ta and Nb concentrations can be attributed to nano- to micro-inclusions of Nb–Ta oxide minerals (especially columbite–tantalite).

The Maršíkov–Schinderhübel III granitic pegmatite represents a classic example of a beryl–columbite granitic pegmatite affected by extensive metamorphic overprinting. The first prograde stage of this metamorphism produced chrysoberyl, quartz, sillimanite muscovite at the expense of primary magmatic beryl, albite and muscovite at amphibolite-facies conditions ($\sim 600^\circ\text{C}$ and 250 –

**Figure 9.** Micro-Raman spectrum of bertrandite with admixture of euclase from the Maršíkov–Schinderhübel III pegmatite.

500 MPa). The subsequent second retrograde stage, probably related to fluid activity along the fault system, resulted in partial alteration of chrysoberyl and crystallisation of secondary Fe-rich beryl, euclase, bertrandite and late muscovite at low-grade conditions (~200–500°C and ≤250 MPa).

Compositions, mineral assemblages and textural relationships of the Be minerals from the Maršíkov–Schinderhübel III granitic pegmatite support the concept that they might serve as useful geochemical and petrological mineral indicators of the conditions of their formation (Barton and Young, 2002; Černý, 2002; Franz and Morteani, 2002; Grew, 2002).

Acknowledgements. Constructive comments from Pietro Vignola, an anonymous reviewer, Associate Editor Edward Grew and Principal Editor Roger Mitchell greatly improved the manuscript. The research was supported by the Ministry of Education, Science, Research and Sport of the Slovak Republic (grant number APVV-18-0065); Comenius University in Bratislava (grant numbers: UK/27/2021 and UK/172/2022); the Ministry of Education, Youth and Sport of the Czech Republic (grant number SGS SP2023/089); and the research project GAČR P210/19/05198S to M. Novák.

Supplementary material. The supplementary material for this article can be found at <https://doi.org/10.1180/mgm.2023.22>.

Competing interests. The authors declare none.

References

- Barton M.D. (1986) Phase equilibria and thermodynamic properties of minerals in the BeO–Al₂O₃–SiO₂–H₂O (BASH) system, with petrologic applications. *American Mineralogist*, **71**, 277–300.
- Barton M.D. and Young S. (2002) Non-pegmatitic deposits of beryllium: mineralogy, geology, phase equilibria and origin. Pp. 591–691 in: *Beryllium: Mineralogy, Petrology and Geochemistry* (E.S. Grew, editor). Reviews in Mineralogy and Geochemistry, **50**. Mineralogical Society of America, Washington DC.
- Burlen H., Thomas R., Melgarejo J.C., Da Silva J.M.R., Rhede D., Soares D.R. and Da Silva M.R.R. (2013) Chrysoberyl-sillimanite association from the Roncadeira pegmatite, Borborema province, Brazil: Implications for gemstone exploration. *Journal of Geosciences*, **58**, 79–90.
- Cempírek J. and Novák M. (2006). Mineralogy of dumortierite-bearing abyssal pegmatites at Starkoč and Běstvina, Kutná Hora Crystalline Complex. *Journal of Geosciences*, **51**, 259–270.
- Černý P. (2002) Mineralogy of beryllium in granitic pegmatites. Pp. 405–444 in: *Beryllium: Mineralogy, Petrology and Geochemistry* (E.S. Grew, editor). Reviews in Mineralogy and Geochemistry, **50**. Mineralogical Society of America, Washington DC.
- Černý P. and Ercit T.S. (2005) The classification of granitic pegmatites revisited. *The Canadian Mineralogist*, **43**, 2005–2026.
- Černý P., Novák M. and Chapman R. (1992) Effects of sillimanite-grade metamorphism and shearing on Nb-Ta oxide minerals in granitic pegmatites: Maršíkov, Northern Moravia, Czechoslovakia. *The Canadian Mineralogist*, **30**, 699–718.
- Černý P., Novák M. and Chapman R. (1995) The Al(Nb,Ta)Ti₂ substitution in titanite: the emergence of a new species? *Mineralogy and Petrology*, **52**, 61–73.
- Cháb J., Fediuková E., Fišera M., Novotný P. and Opletal M. (1990) Variscan orogeny in Silesicum. *Sborník Geologických Věd, Ložisková Geologie, Mineralogie*, **29**, 9–39 [in Czech, English summary].
- Cháb J., Stráňák Z. and Eliáš M. (2007) *Geological map of Czech Republic 1 : 500 000 (uncovered)*. Czech Geological Survey, Prague.
- Chládek Š. and Zimák J. (2016) Association of Nb-Ta-(Ti-REE) oxide minerals in the Maršíkov–Lysá Hora pegmatite in Hrubý Jeseník Mountains, Czech Republic. *Bulletin Mineralogie Petrologie*, **24**, 25–32 [in Czech, English abstract].
- Chládek Š., Uher P. and Novák M. (2020) Compositional and textural variations of columbite-group minerals from beryl-columbite pegmatites in the Maršíkov District, Bohemian Massif, Czech Republic: Magmatic versus hydrothermal evolution. *The Canadian Mineralogist*, **58**, 767–783.
- Chládek Š., Uher P., Novák M., Bačík P., and Opletal T. (2021) Microlite-group minerals: tracers of complex post-magmatic evolution in beryl-columbite granitic pegmatites, Maršíkov District, Bohemian Massif, Czech Republic. *Mineralogical Magazine*, **85**, 725–743.
- Colombo F., Sfragulla J., González del Tánago J. and Pannunzio Miner E. (2021) Chrysoberyl from the Tablata I pegmatite, Pocho pegmatitic Group, Altautina district (Córdoba province, Argentina). *Revista de la Asociación Geológica Argentina*, **78**, 344–354 [in Spanish, English abstract].
- Dixon A., Cempírek J. and Groat L.A. (2014) Mineralogy and geochemistry of pegmatites on Mount Begbie, British Columbia. *The Canadian Mineralogist*, **52**, 129–164.
- Dolníček Z., Nepejchal M., Sejkora J., Ulmanová J. and Chládek Š. (2020a) Bohseite from beryl-columbite pegmatite D6e in Maršíkov (Silesicum, Czech Republic). *Bulletin Mineralogie Petrologie*, **28**, 219–223 [in Czech, English summary].
- Dolníček Z., Nepejchal M. and Novák M. (2020b) Minerals of the bavenite-bohseite series from the Schinderhübel I pegmatite in Maršíkov (Silesicum, Czech Republic). *Bulletin Mineralogie Petrologie*, **28**, 353–358 [in Czech, English summary].
- Dostál J. (1966) Mineralogical and petrographical conditions of the chrysoberyl-sillimanite pegmatite from Maršíkov. *Acta Universitatis Carolinae, Geologica*, **4**, 271–287 [in German].
- Dostál J. (1969) Some new data for chrysoberyl from Maršíkov, Northern Moravia. *Acta Universitatis Carolinae – Geologica*, **4**, 261–287.
- Downes P.J. and Bevan A.W.R. (2002) Chrysoberyl, beryl and zincian spinel mineralization in granulite-facies Archaean rocks at Dowerin, Western Australia. *Mineralogical Magazine*, **66**, 985–1002.
- Franz G. and Morteani G. (1981) The system BeO–Al₂O₃–SiO₂–H₂O: Hydrothermal investigation of the stability of beryl and euclase in the range from 1 to 6 kb and 400 to 800°C. *Neues Jahrbuch für Mineralogie, Abhandlungen*, **140**, 273–299.
- Franz G. and Morteani G. (1984) The formation of chrysoberyl in metamorphosed pegmatites. *Journal of Petrology*, **25**, 27–52.
- Franz G. and Morteani G. (2002) Be-minerals: synthesis, stability, and occurrence in metamorphic rocks. Pp. 551–589 in: *Beryllium: Mineralogy, Petrology and Geochemistry* (E.S. Grew, editor). Reviews in Mineralogy and Geochemistry, **50**. Mineralogical Society of America, Washington DC.
- Galliski M.Á., Márquez-Zavalía M.F., Lira R., Cempírek J. and Škoda R. (2012) Mineralogy and origin of the dumortierite-bearing pegmatites of Virorco, San Luis, Argentina. *The Canadian Mineralogist*, **50**, 873–894.
- Grew E.S. (1981) Surinamite, taaffeite, and beryllian sapphire from pegmatites in granulite-facies rocks in Casey Bay, Enderby Land, Antarctica. *American Mineralogist*, **66**, 1022–1033.
- Grew E.S. (2002) Beryllium in metamorphic environments (emphasis on aluminous compositions). Pp. 487–549 in: *Beryllium: Mineralogy, Petrology and Geochemistry* (E.S. Grew, editor). Reviews in Mineralogy and Geochemistry, **50**. Mineralogical Society of America, Washington DC.
- Hawthorne F.C. and Huminicki D.M.C. (2002) The crystal chemistry of beryllium. Pp. 333–403 in: *Beryllium: Mineralogy, Petrology and Geochemistry* (E.S. Grew, editor). Reviews in Mineralogy and Geochemistry, **50**. Mineralogical Society of America, Washington DC.
- Hazen R.M. and Finger L.W. (1987) High-temperature crystal chemistry of phenakite (Be₂SiO₄) and chrysoberyl (BeAl₂O₄). *Physics and Chemistry of Minerals*, **14**, 426–434.
- Hegner E. and Kröner A. (2000) Review of Nd isotopic data and xenocrystic and detrital zircon ages from the pre-Variscan basement in the eastern Bohemian Massif: Speculations on palinspastic reconstructions. *Geological Society Special Publication*, **179**, 113–129.
- Hong T., Zhai M.-G., Xu X.-W., Li H., Wu C., Ma Y.-C., Niu L., Ke Q. and Wang C. (2021) Tourmaline and quartz in the igneous and metamorphic rocks of the Tashisayi granitic batholith, Altyn Tagh, northwestern China: Geochemical variability constraints on metallogenesis. *Lithos*, **400–401**, 106358.
- Hruschka W. (1824) Occurrence and crystallization of the Moravian fossils. 1. Chrysoberyl. *Mittheilungen der k. k. Mährisch-Schlesischen Gessellschaft zur Beförderung des Ackerbaues, der Natur- und Landeskunde in Brünn*, **52**, 413–415 [in German].

- Janoušek V., Aichler J., Hanžl P., Gerdes A., Erban V., Žáček V., Pecina V., Pudilová M., Hrdličková K., Mixa P. and Žáčková E. (2014) Constraining genesis and geotectonic setting of metavolcanic complexes: A multidisciplinary study of the Devonian Vrbno Group (Hrubý Jeseník Mts., Czech Republic). *International Journal of Earth Sciences*, **103**, 455–483.
- Jastrzębski M., Żelaźniewicz A., Sláma J., Machowiak K., Śliwiński M., Jaźwa A. and Kocjan I. (2021) Provenance of Precambrian basement of the Brunovistulian Terrane: New data from its Silesian part (Czech Republic, Poland), central Europe, and implications for Gondwana break-up. *Precambrian Research*, **355**, 106108.
- Kanouo N.S., Ekomane E., Youngue R.F., Njonfang E., Zaw K., Changqian M., Ghogomu T.R., Lentz D.R. and Venkatesh A.S. (2016) Trace elements in corundum, chrysoberyl, and zircon: Application to mineral exploration and province study of the western Mamfe gem clastic deposits (SW Cameroon, Central Africa). *Journal of African Earth Sciences*, **113**, 35–50.
- Košulíková M. and Štípská P. (2007) Variations in the transient prograde geothermal gradient from chloritoid-staurolite equilibria: A case study from the Barrovian and Buchan-type domains in the Bohemian Massif. *Journal of Metamorphic Geology*, **25**, 19–36.
- Kretschmer F. (1911) Chrysoberyl from Marschendorf and its association. *Tschermaks Mineralogische und Petrographische Mitteilungen*, **30**, 85–103 [in German].
- Kröner A., Štípská P., Schulmann K. and Jaekel P. (2000) Chronological constraints on the pre-Variscan evolution of the northeastern margin of the Bohemian Massif, Czech Republic. *Geological Society, London, Special Publication*, **179**, 175–197.
- Lafuente B., Downs R.T., Yang H. and Stone N. (2016) The power of databases: The RRUFF project. *Highlights in Mineralogical Crystallography*, **10**, 1–29.
- Laurent A., Janoušek V., Magna T., Schulmann K. and Míková J. (2014) Petrogenesis and geochronology of a post-orogenic calc-alkaline magmatic association: The Žulová Pluton, Bohemian Massif. *Journal of Geosciences*, **59**, 415–440.
- Lira R. and Sfragulla J. (2011) Granitic pegmatite chrysoberyl in a shear zone of the Achala Batholith, Córdoba, Argentina. *Asociación Geológica Argentina*, **14**, 127–130.
- Lupulescu M.V., Chiarenzelli J.R. and Bailey D.G. (2012) Mineralogy, classification, and tectonic setting of the granitic pegmatites of New York State, USA. *The Canadian Mineralogist*, **50**, 1713–1728.
- Marschall D. and Walton L. (2014) Chrysoberyl. Pp. 207–215 in: *Geology of Gem Deposits. Second Edition* (L.A. Groat, editor). Mineralogical Association of Canada, Short Course Series, **44**. Mineralogical Association of Canada, Québec.
- Martin-Izard A., Paniagua A. and Moreiras D. (1995) Metasomatism at a granitic pegmatite – dunite contact in Galicia: the Franqueira occurrence of chrysoberyl (alexandrite), emerald, and phenakite. *The Canadian Mineralogist*, **33**, 775–792.
- Merino E., Villaseca C., Orejana D. and Jeffries T. (2013) Gahnite, chrysoberyl and beryl co-occurrence as accessory minerals in a highly evolved peraluminous pluton: The Belvís de Monroy leucogranite (Cáceres, Spain). *Lithos*, **179**, 137–156.
- Mikulski S.Z., Williams I.S. and Bagiński B. (2013) Early Carboniferous (Viséan) emplacement of the collisional Klodzko-Złoty Stok granitoids (Sudetes, SW Poland): Constraints from geochemical data and zircon U–Pb ages. *International Journal of Earth Sciences*, **102**, 1007–1027.
- Novák M. (1988) Garnets from pegmatites of the Hrubý Jeseník (Northern Moravia). *Acta Musei Moraviae Scientiae Naturales*, **73**, 3–28 [in Czech, English summary].
- Novák M. (2005) Granitic pegmatites of the Bohemian Massif (Czech Republic); mineralogical, geochemical and regional classification and geological significance. *Acta Musei Moraviae Scientiae Geologicae*, **90**, 3–74. [in Czech, English summary].
- Novák M. and Rejl L. (1993) Relationship between muscovite pegmatites and geophysical fields at the Hrubý Jeseník area. *Acta Musei Moraviae Scientiae Naturales*, **77**, 49–61 [in Czech, English summary].
- Novák M., Černý P. and Uher P. (2003) Extreme variation and apparent reversal of Nb-Ta fractionation in columbite-group minerals from the Scheibengraben beryl-columbite granitic pegmatite, Marsikov, Czech Republic. *European Journal of Mineralogy*, **15**, 565–574.
- Novák M., Dolníček Z., Zachař A., Gadas P., Nepejchal M., Sobek K., Škoda R. and Vrtiška L. (2023) Mineral assemblages and compositional variations in bavenite–bohseite from granitic pegmatites of the Bohemian Massif, Czech Republic. *Mineralogical Magazine*, **87**, <https://doi.org/10.1180/mgm.2023.17>
- Pautov L.A., Popov M.P., Erokhin Y. V., Khiller V. V and Karpenko V.Y. (2013) Mariinskite, BeCr₂O₄, a new mineral, chromium analog of chrysoberyl. *Geology of Ore Deposits*, **55**, 648–662.
- René M. (1983) Geochemistry and petrology of metapelites in the envelope of the core of the Desná Dome in northern Moravia. *Časopis pro mineralogii a geologii*, **28**, 277–286. [in Czech].
- Schmetzer K., Caucia F., Gilg H.A. and Coldham T.S. (2016) Chrysoberyl recovered with sapphires in the New England placer deposits, New South Wales, Australia. *Gems and Gemology*, **52**, 18–36.
- Schulmann K. and Gayer R. (2000) A model for a continental accretionary wedge developed by oblique collision: the NE Bohemian Massif. *Journal of the Geological Society, London*, **157**, 401–416.
- Schulmann K., Olliot E., Košulíková M., Montigny R. and Štípská P. (2014) Variscan thermal overprints exemplified by U–Th–Pb monazite and K–Ar muscovite and biotite dating at the eastern margin of the Bohemian Massif (East Sudetes, Czech Republic). *Journal of Geosciences*, **59**, 389–413.
- Soman K. and Nair N.G.K. (1985) Genesis of chrysoberyl in the pegmatites of southern Kerala, India. *Mineralogical Magazine*, **49**, 733–738.
- Souček J. (1978) Metamorphic zones of the Vrbno and Rejvíz series, the Hrubý Jeseník Mountains, Czechoslovakia. *Tschermaks Mineralogische und Petrographische Mitteilungen*, **25**, 195–217.
- Staněk J. (1981) Pegmatites of Moravia. Pp. 132–174. in: *Mineralogie Československa* (J.H. Bernard, editor). Academia, Praha [in Czech].
- Sun Z., Palke A.C., Muyal J., DeGhionno D. and McClure S.F. (2019) Geographic origin determination of alexandrite. *Gems and Gemology*, **55**, 660–681.
- Vignola P., Zucali M., Rotiroti N., Marotta G., Risplendente A., Pavese A., Boscardin M., Mattioli V. and Bertoldi G. (2018) The chrysoberyl- and phosphate-bearing albite pegmatite of Malga Garbella, Val di Rabbi, Trento Province, Italy. *The Canadian Mineralogist*, **56**, 411–424.
- Warr L.N. (2021) IMA–CNMNC approved mineral symbols. *Mineralogical Magazine*, **85**, 291–320.
- Žáček V. and Vrána S. (2002) Iron-rich chrysoberyl from Kalanga Hill, Muyombe District, north-eastern Zambia. *Neues Jahrbuch für Mineralogie Monatshefte*, **2002**, 529–540.